

Path-Integral Calculations of Normal Liquid ^3He

D. M. Ceperley

*Department of Physics and National Center for Supercomputing Applications, University of Illinois at Urbana-Champaign,
1110 West Green Street, Urbana, Illinois 61801*

(Received 14 February 1992)

The first path-integral calculations of the properties of a strongly correlated continuum fermion system are described. The paths are restricted to the region of phase space with a positive trial density matrix, thereby avoiding the fermion sign problem. This restriction is exact if the nodes of the trial density matrix are correctly placed, but otherwise gives a physically reasonable approximation generalizing the "fixed-node" approximation used at zero temperature. Computations show that restricting the walks with the noninteracting density matrix gives good results for liquid ^3He above 1 K. Using imaginary-time-independent nodes or not allowing atomic exchange results in substantially poorer agreement with experimental energies.

PACS numbers: 67.50.Dg, 61.20.Ja, 71.10.+x

This Letter describes a new computational method applicable to strongly correlated many-fermion systems at nonzero temperature such as liquid ^3He for $T \geq 0.5$ K where both degeneracy effects and temperature are significant. Feynman [1] introduced an exact mapping of superfluid ^4He onto a classical system of "ring polymer" particles. This formalism has been used to implement a powerful path-integral Monte Carlo method (PIMC) [2,3] for Bose systems. The lambda transition, superfluidity, and momentum condensation are mirrored by the formation of a macroscopic exchange of the paths. Good agreement between simulations and experiment has been achieved in both bulk and liquid ^4He films. We wish to generalize this intuitive and powerful approach to fermion systems.

Previous simulations of liquid ^3He have calculated ground-state properties with the variational Monte Carlo (VMC) and Green's-function Monte Carlo (GFMC) methods. VMC [4] calculates properties of a known trial function, while the potentially exact GFMC [5] method uses the Hamiltonian to project out the lowest-energy state with a branching random walk, but it converges very slowly for large numbers of fermions [6]. Neverthe-

less, agreement with the experimental binding energy has been obtained with extensive transient estimate calculations of 54 atoms [7,8]. We note that the hard repulsion between two He atoms cannot be transformed into an integral over an auxiliary field as is done for lattice models.

Because of the slow convergence of GFMC for fermions, the fixed-node approximation (FN) has been introduced [9], where the effect of the fermion sign is only approximately taken into account. The diffusion of the branching random walks is constrained to remain on one side of the nodes of a given antisymmetric trial function, thus determining the best upper bound to the energy consistent with a given set of nodes [10]. In fact, the energy is not very sensitive to the node locations if their location is at all reasonable. For example, with free particle nodes one obtains a binding energy of -1.90 K for liquid ^3He , and with the backflow nodes [8] -2.37 K, only 0.1 K above the experimental value. Calculations of properties other than the energy are substantially more difficult than in the path-integral method and are necessarily limited to zero temperature.

To make the fixed-node approximation for path integrals consider the imaginary-time path-integral expression for the many-body density matrix [1]

$$\rho(R, R_0; \beta) = C \sum_P (-1)^P \int_{PR_0}^R dR \exp \left\{ - \int_0^\beta dt \left[\frac{1}{4\lambda} \left(\frac{dR}{dt} \right)^2 + V(R(t)) \right] \right\}, \quad (1)$$

where the integral dR is over all continuous paths starting at PR_0 and ending at R , P is a permutation of atoms with the same spin, $V(R)$ is the potential energy, $\lambda = \hbar^2/2m$, and C is a constant. The integration variable t will be called "time," and R refers to the $3N$ -dimensional vector of atomic coordinates. One uses this expression for the path-integral Monte Carlo method [2,11] by dividing up the time integral into a discrete number of time slices, t_k , finding the most accurate expression for the density matrix within each time slice, and sampling the variables $R(t_k)$ and P .

For fermions, this expression is not useful at low temperatures or for large systems because the sign of the permutation must be included as a weight; the contribution from even permutations is only very slightly larger than the contribution from odd permutations. At low temperatures any expectation will be proportional to $e^{-\beta E_F}$ for fermions but $e^{-\beta E_B}$ for unsigned paths where E_F and E_B are the boson and fermion ground-state energies. This implies that the signal/noise ratio of the "unrestricted" PIMC for fermion systems approaches $e^{-\beta(E_F - E_B)}$ at low

temperatures; the exponent grows linearly in *both* β and N , the number of fermions.

To derive the identity on which the FN-PIMC method is based, recall that the exact fermion density matrix is a solution to

$$-\frac{d\rho(R, R_0; t)}{dt} = \left[-\lambda \sum_i \nabla_i^2 + V(R) \right] \rho(R, R_0; t) \quad (2)$$

with the initial condition

$$\rho(R, R_0; 0) = \sum_P \frac{(-1)^P}{N! N!} \delta(R - PR_0). \quad (3)$$

An infinite potential barrier can be placed at the nodes of $\rho(R, R_0; t)$ without changing the solution because Eq. (2) is uniquely determined by its boundary conditions. Instead of boundary conditions only at $\beta=0$, we can use the surface of a nodal region of $\rho(R, R_0; t)$ to enforce antisymmetry. These nodal regions are in a space of dimension $3N+1$ if we consider R_0 fixed. The barriers are simply a way of requiring that the density matrix vanish at the boundary and are easily treated by path integrals; the paths are *restricted* to remain inside a single nodal region of ρ . Paths which cross the nodes can be eliminated because the gradient of the density matrix is proportional to the flux of unrestricted paths and the flux of positive paths cancels the flux of negative paths at the node.

The restricted-path-integral equation is identical to Eq. (1) but the integral is only over paths with $\rho(R(t), R_0; t) \neq 0$. The exact density matrix will then appear both on the left-hand side of Eq. (1) and implicitly in the limits of the integrand on the right-hand side. In the fixed-node approximation, a trial density matrix is used for the restriction on the right-hand side.

The permutation sum still appears in the path-integral expression, but for calculations of the diagonal density matrix, where $R(\beta) = PR(0)$, paths starting at an odd permutation will clearly have to cross the nodes and so are excluded. Hence the sign of any path needed in the evaluation of the diagonal density matrix is always positive. Nontrivial even permutations are allowed and we will see that they make an important contribution at low temperatures.

Boson path integrals possess a symmetry under time translations: The probability distribution of any point, $R(t)$, on the path is proportional to the diagonal density matrix which implies that any time slice can be taken as the time origin. The restricted fermion paths do not have this symmetry. The point R_0 , which we will call the *reference point*, defines the nodes and only it will have the probability distribution of the diagonal density matrix. Other time slices on the path will have a different distribution. Boson path integrals have an action which is local in time but the restricted fermion action is nonlocal in time and "time dependent."

Before we discuss the trial density matrix, there is a simple way of improving any nodal approximation: Two

reference points, at times 0 and $\beta/2$, can be used as easily as one. Then we only need the nodes of the trial density matrix for times $t \leq \beta/2$. If more reference points were used or if the second reference point would have a time argument other than $\beta/2$, it would be possible to have negative paths. Evaluations of scalar quantities such as the pair-correlation function or the potential energy are performed by averaging only over the two reference points.

Our calculations have used two different trial density matrices: the exact noninteracting density matrix (NI),

$$\rho_{\text{NI}}(R, R_0; \beta) = [4\lambda\beta\pi]^{-3N/2} \det[e^{-(r_i - r_{j0})^2/4\lambda\beta}] \quad (4)$$

and the ground-state noninteracting wave function (GS),

$$\rho_{\text{GS}}(R, R_0; \beta) = \det[e^{i\mathbf{k}_i \cdot \mathbf{r}_j}], \quad (5)$$

where $\{\mathbf{k}_i\}$ is a set of occupied momentum states.

One can demonstrate [12] that the nodes of a correlated density matrix approach those of the NI density matrix in the classical limit, $\beta \rightarrow 0$. The NI nodes are both time dependent and R_0 dependent (except in 1D). On the other hand, the GS nodes are independent of both R_0 and β which makes them computationally convenient but less accurate.

In these noninteracting density matrices there are separate determinants for spin-up and spin-down atoms. This implies the paths are restricted to have both an even $P\uparrow$ and an even $P\downarrow$. It is known that nodes with backflow correlation [7] describe liquid ^3He much more accurately and presumably would allow odd-odd permutations. However, their use in PIMC, while feasible [12], is significantly more complicated and has not yet been implemented.

Monte Carlo calculations using restricted path integrals have been carried out for 38 and 66 ^3He atoms in a periodic box at the zero-pressure density of $0.016355/\text{\AA}^3$ and interacting with the phenomenological Aziz-2 [13] potential. The computer calculations are several times longer than an equivalent boson calculation. Some new features of the fermion simulation are the following.

When time is discretized, it is best to choose an accurate action so that the time step can be chosen as large as possible. Reference [11] discusses the use of the exact two-body density matrix in the term of the action corresponding to the potential. It is also important to treat carefully the restriction because it has the form of a hard wall. If one assumes the nodes are locally planar, it is easy to find the exact action as the probability that the path does not cross the nodes within a time slice. We have tested that the energy is converged to better than 0.1 K/atom with a time step of $\tau = 0.0125/\text{K}$, half the time step used in liquid ^4He .

The method for moving in path and permutation space is a generalization of that used for boson superfluids [11], the bisection method. There are three types of moves in

this Metropolis procedure. Some moves consist of the resampling of a single atom's position in fifteen adjacent time slices. Occasionally an attempt is made to insert a cyclic permutation of three adjacent atoms in fifteen adjacent time steps and thereby move around in even permutation space. Note that if the reference point is moved, the action for all the other time slices will change, because their nodal distances change. Surprisingly, the acceptance ratio remains high for this type of move.

Finally, moves are made of the reference point by simply shifting the time labeling. This only affects the fermion part of the action. The acceptance ratio for these reference moves varied from 86% at 3 K, to 1% at 1 K. It seems that the nodes of the density matrix are "rotating" as β increases so that for temperatures lower than 1 K the restricted paths are pinned with respect to a reference re-labeling. But at these low temperatures the single- and three-particle moves remain effective in moving the reference point. The code was tested against exact results for noninteracting fermions.

Figure 1 shows the internal energies as computed with FN-PIMC for 38 atoms and compared with experiment. Shown are four sets of results corresponding to the two nodal choices and using only the identity permutation (*I*) or allowing a full sampling of the even permutation space

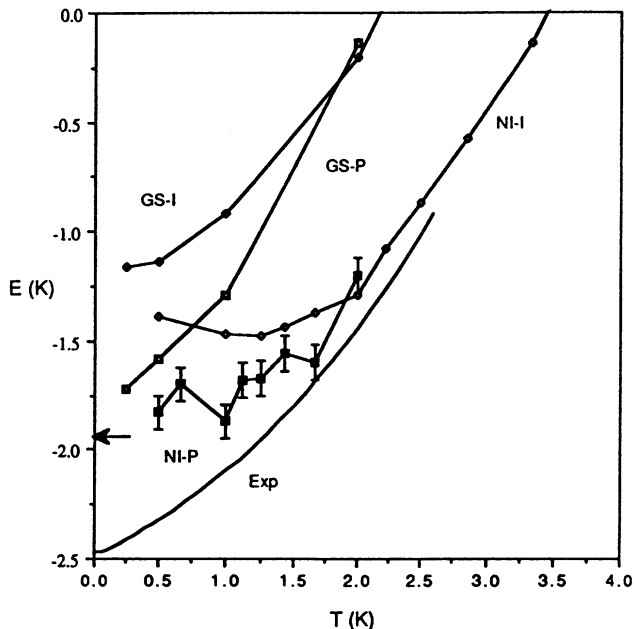


FIG. 1. The energy of liquid ${}^3\text{He}$ vs temperature at a density of $0.016355/\text{\AA}^3$ (near zero pressure). The line represents the experimental data [14]. The symbols are the PIMC calculations for 38 atoms using GS nodes and permutations (GS-*P*) and without permutations (GS-*I*), and the NI nodes with and without permutations (NI-*P* and NI-*I*). The statistical error for each MC point is 0.05 K. The arrow shows the result at zero temperature as computed by GFMC, also for 38 atoms, with GS nodes.

(*P*). All four curves must converge to the FN-GFMC result of -1.9 K/atom but their behavior as a function of temperature is quite distinctive.

Consider first the use of the GS nodes. Although GS nodes are computationally simpler, they significantly raise the energy, except at the very lowest temperature. The number of atoms was chosen so that the noninteracting ground state is nondegenerate and thus the NI nodes must go over to the GS nodes at temperatures significantly lower than the gap to the first excited state of 1.8 K. But we see that the time dependence inherent in the NI nodes is very important for all temperatures $T \geq 0.5$ K.

Next consider the importance of even permutations. Without permutations, the energy does not approach the correct low-temperature limit of 1.9 K, either in the NI or the GS case. Apparently it will take a much lower temperature for these nonexchanging fermions to stretch out to the lower kinetic-energy conformations. There is a very strong even-odd effect in the permutation statistics for $T > 1$ K; the density of exchanges is sufficiently low that it matters whether a given cycle is composed of an even or odd number of atoms. But by 0.5 K the cycle length distribution is approaching a constant indicating that the occupation of the even permutation space is approaching a uniform distribution. The temperature at which macroscopic exchanges become likely is an order of magnitude lower than it would be for Bose ${}^3\text{He}$ because of the restriction.

The NI-*P* energies are in good agreement with experiment (as they should be) for temperatures greater than 1 K. Effects of finite system size and interatomic potential could account for the differences between the FN and experimental results for $T \geq 1$ K. For temperatures less than 2 K the energies of 66 atoms are about 0.1 K higher than for 38 atoms, indicating finite-size effects are about 0.1 K, consistent with what is found at zero temperature. The pair-correlation functions and static structure factors are also in good agreement with experimental measurements. The potential energy changes only by 0.2 K as the temperature changes from 0.5 to 4 K and is insensitive to the trial density matrix. The dramatic changes in the low-temperature properties are due to opening up of regions of phase space as the paths lengthen, which is reflected in the kinetic energy alone.

In this paper we have introduced a restriction for fermion path integrals and shown that it leads to reasonable results for liquid ${}^3\text{He}$ with free particle nodes. The introduction of an approximation for the nodes could lead to systematic errors, but, nonetheless, we believe the method will be very useful. Consider the analogy with a classical protein. To perform an exact simulation of a protein one needs the exact electronic energy for an arbitrary conformation of the protein, a $3N$ -dimensional function. In practice, an empirical energy function with the correct geometry and charge distributions is sufficient to describe generic features of protein conformations and motions,

and to aid in the interpretation of experiments. We argue that an ansatz for the nodes, a $(6N+1)$ -dimensional function, is similar, but in many ways under better control. The approximation only restricts the region of phase space where paths are allowed; the action inside those volumes is exactly known. The nodes must satisfy known constraints, such as be symmetrical, approach the classical high-temperature limit, smoothly evolve from the high- T to ground-state limit, etc. It is likely that there are variational or self-consistent principles for the nodes which can be used to improve them.

In any case, since there exists an *exact* "classical analogy" for fermion systems, similar to the one Feynman introduced for Bose superfluids, we can ask for the manifestations of the superfluid phase of liquid ^3He . For the unrestricted signed paths, the superfluid density is related to the difference between the mean-squared winding of even and odd exchanges [15]. The calculation of the superfluid density with restricted paths is more complicated since one needs a two-time correlation function requiring two reference points which can bring in minus signs. In our tests, winding around the periodic boundaries was observed for temperatures at or below 2 K but we have not yet evaluated the superfluid density. It is unclear whether pairing is a generic property of any proper nodes, such as those with backflow correlation, or whether subtle changes in the topology of the nodal regions are involved in the phase transition. The classical analogy of restricted paths provides an interesting alternative picture to BCS theory and may lead to the possibility of calculating the transition temperatures of superfluids and superconductors.

Even if FN-PIMC is not successful in calculating superfluid properties of fermions, either because the nodes are too complicated or because it is too difficult to move the paths in the low-temperature limit, this method should be effective in determining properties of interacting fermion systems at higher temperatures.

I thank E. L. Pollock, J. Theilhaber, B. Bernu, M.

Wagner, and S. Bacci for useful discussions. This work was supported by the National Science Foundation through Grant No. NSF DMR88-08126. The computations used the Cray-YMP and the IBM RS-6000 workstations at the National Center for Supercomputing Applications.

-
- [1] R. P. Feynman, Phys. Rev. **90**, 1116 (1953); R. P. Feynman and A. R. Hibbs, *Quantum Mechanics and Path Integrals* (McGraw-Hill, New York, 1965).
 - [2] E. L. Pollock and D. M. Ceperley, Phys. Rev. B **30**, 2555 (1984).
 - [3] D. M. Ceperley and E. L. Pollock, Phys. Rev. Lett. **56**, 351 (1986).
 - [4] D. M. Ceperley, G. V. Chester, and M. H. Kalos, Phys. Rev. B **16**, 3081 (1977).
 - [5] D. M. Ceperley and M. H. Kalos, in *Monte Carlo Methods in Statistical Physics*, edited by K. Binder (Springer-Verlag, Berlin, 1979).
 - [6] K. E. Schmidt and M. H. Kalos, in *Monte Carlo Methods in Statistical Physics II*, edited by K. Binder (Springer-Verlag, Berlin, 1984).
 - [7] K. E. Schmidt, M. H. Kalos, M. A. Lee, and G. V. Chester, Phys. Rev. Lett. **45**, 573 (1980).
 - [8] R. M. Panoff and J. Carlson, Phys. Rev. Lett. **62**, 1130 (1989).
 - [9] J. B. Anderson, J. Chem. Phys. **63**, 1499 (1975); **65**, 4121 (1976).
 - [10] D. M. Ceperley, in *Recent Progress in Many-Body Theories*, edited by J. Zabolitzky (Springer-Verlag, Berlin, 1981).
 - [11] D. M. Ceperley and E. L. Pollock, in Proceedings of the Elba Conference on Monte Carlo Methods for Physics, 1990 (to be published).
 - [12] D. M. Ceperley, J. Stat. Phys. **63**, 1237 (1991).
 - [13] R. A. Aziz, V. P. S. Nain, J. S. Carley, W. L. Taylor, and G. T. McConville, J. Chem. Phys. **70**, 4330 (1979).
 - [14] D. S. Greywall, Phys. Rev. B **27**, 2747 (1983).
 - [15] E. L. Pollock and D. M. Ceperley, Phys. Rev. B **36**, 8343 (1987).